

Short Note

Turbulent channel flow simulations in convecting reference frames

M. Bernardini^{a,*}, S. Pirozzoli^a, M. Quadrio^b, P. Orlandi^a^a Dipartimento di Ingegneria Meccanica e Aerospaziale, via Eudossiana 18, 00184 Roma, Italy^b Dipartimento di Ingegneria Aerospaziale, Politecnico di Milano, via La Masa 34, 20156 Milano, Italy

ARTICLE INFO

Article history:

Received 8 February 2012

Received in revised form 25 July 2012

Accepted 7 August 2012

Available online 23 August 2012

Keywords:

Turbulent channel flow
Finite-difference method
Galilean invariance

ABSTRACT

We perform finite-difference numerical simulations of turbulent channel flow in stationary and moving reference frames. The flow statistics computed in the stationary frame exhibit significant discrepancies with respect to reference spectral data in terms of energy spectra and convection velocity of disturbances, especially in the near-wall region. On the other hand, simulations performed in a reference frame moving with the bulk flow velocity suffer from this shortcoming to a much lesser extent. We propose an explanation of these observations by assuming the scalar Burgers' equation as working model. The analysis highlights the lack of Galilean invariance of finite-difference schemes, which exhibit a leading dispersive error in the presence of bulk advection. The numerically computed energy spectra exhibit the same features as the channel spectra, supporting the notion that dispersive effects are responsible for the blockage of the mechanism of energy cascade to high wavenumbers.

© 2012 Elsevier Inc. All rights reserved.

1. Introduction

In the past decades significant insight into turbulence physics has been gained through direct numerical simulation (DNS), which has become an invaluable research tool for the fluid dynamics community [1]. One of the most investigated (and simulated) turbulent flows is the plane channel, which, together with the pipe flow, is the simplest prototype to understand wall turbulence. Since the first DNS, dating back to the work of Kim et al. [2], many simulations of the turbulent channel flow have appeared during the years, performed with both spectral and finite-difference (FD) methods [3,4]. The comparison between the two approaches has been addressed in several works [5–7], which have pointed out relative advantages and deficiencies. Spectral methods are known to suffer particularly from the aliasing error, which has to be carefully removed from the computation, but they are usually regarded to be more accurate, an often quoted result being that second-order central difference schemes require about twice the resolution in each coordinate direction to achieve similar results. On the other hand FD methods have lower level of aliasing errors [7] and they are attractive for their inherent simplicity and flexibility, especially for inhomogeneous flows, and their relative importance might further increase owing to the rapid development of the immersed-boundary technique to deal with complex geometries.

One drawback of FD methods for the Navier–Stokes (NS) equations, appears when dealing with turbulent flows that have a convective character and thus possess a preferential direction of propagation of disturbances. This happens, for example, in duct flows, boundary layers and jets. In this case, if the grid is not sufficiently fine, FD methods yield a misrepresentation of the small scales of motion (in the direction of flow propagation), which manifests itself in non-negligible errors in the prediction of the short wavelength disturbances, whose energy and phase velocity are underestimated. The aim of the paper is to trace back the origin of this behavior, and suggest a solution to reduce these errors. To provide an instance of the effects

* Corresponding author. Tel.: +39 0644585285.

E-mail address: matteo.bernardini@uniroma1.it (M. Bernardini).

Table 1
Computational parameters for the channel flow simulations.

Case	Re_τ	L_x/h	L_z/h	Δx^+	Δz^+	N_x	N_y	N_z	Δt^+
Run 1	547	8π	4π	13.4	6.7	1024	256	1024	0.264
Run 2	547	8π	4π	8.9	4.4	1536	256	1536	0.176
Run 3	547	8π	4π	6.7	3.3	2048	256	2048	0.132
Run 4	547	8π	4π	13.4	6.7	1024	256	1024	0.024

described above, we have carried out DNS of the turbulent channel flow at $Re_\tau = 550$, for which a well-documented reference numerical database obtained with spectral methods is available [3]. Here $Re_\tau = hu_\tau/\nu$ is the friction Reynolds number, based on the friction velocity u_τ , the kinematic viscosity ν , and the channel half-width h . A series of simulations, whose parameters are summarized in Table 1, have been performed with the FD code described by Orlandi [8], which relies on staggered second-order central FD approximations. Time advancement is achieved by a hybrid third-order Runge–Kutta/second-order Crank–Nicolson scheme, combined with the fractional-step procedure, with explicit treatment of the convective terms, and implicit treatment of the viscous ones. All the simulations have been carried out in a computational box with size $L_x = 8\pi h$ in the streamwise direction, and $L_z = 4\pi h$ in the spanwise direction, by varying the resolution in the homogeneous directions from a relatively coarse grid (Run 1, $\Delta x^+ = 13.4$, $\Delta z^+ = 6.7$) to a very fine grid (Run 3, $\Delta x^+ = 6.7$, $\Delta z^+ = 3.3$). Note that Run 1 and Run 2 match the resolution of the reference spectral database in terms of number of Fourier modes and physical points, respectively. An additional simulation (Run 4) has been also performed with the same resolution as Run 1, by choosing a reduced time step to assess the influence of the time discretization errors. Note that the time step of all cases is within the range suggested by Choi et al. [5] to get accurate statistics ($\Delta t^+ \leq 0.4$). For all computations, a Chebychev distribution is used in the vertical direction to cluster points near the two walls. The failure of the numerical solver to correctly represent the high-wavenumber disturbances is well highlighted in Fig. 1, where one-dimensional spectra of the streamwise velocity fluctuations are shown in Kolmogorov units, at two off-wall locations. Note that a semi-log scale is used to emphasize the high-wavenumber end of the spectra. The streamwise spectra predicted by the FD method (panels a,c) exhibit much earlier drop-off than the reference spectra in the dissipation range, this effect being particularly apparent in the outer layer. Increasing the resolution improves the comparison but deviations (still large in the outer layer) are observed even for the finest grid. Remarkably, this behavior does not depend on the computational time step, the spectra from Run 1 and Run 4 being nearly identical. A similar behavior of the streamwise velocity spectrum was also previously noticed by Rai and Moin

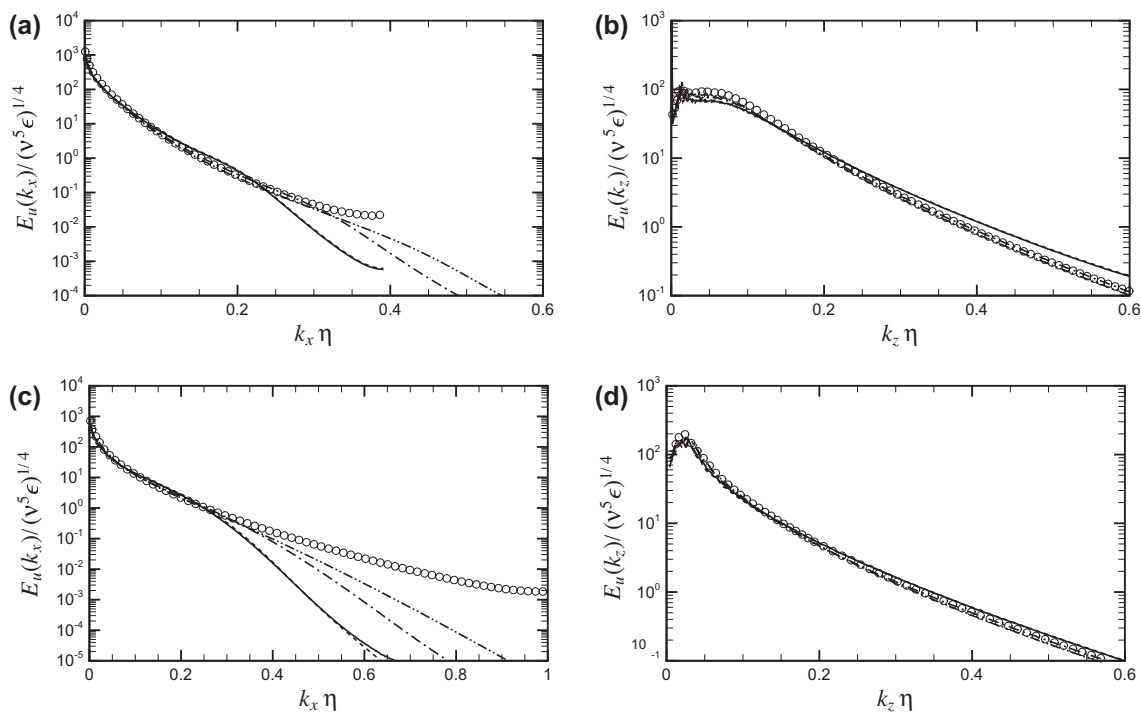


Fig. 1. Channel flow simulations in the laboratory frame: one-dimensional spectral densities of streamwise velocity fluctuations at $y^+ = 15$ (a,b) and $y/h = 0.75$ (c,d), scaled in Kolmogorov units (η). Solid line, Run 1; dash-dot line, Run 2; dash-dot-dot line, Run 3; dashed line, Run 4; open circles, reference data [3].

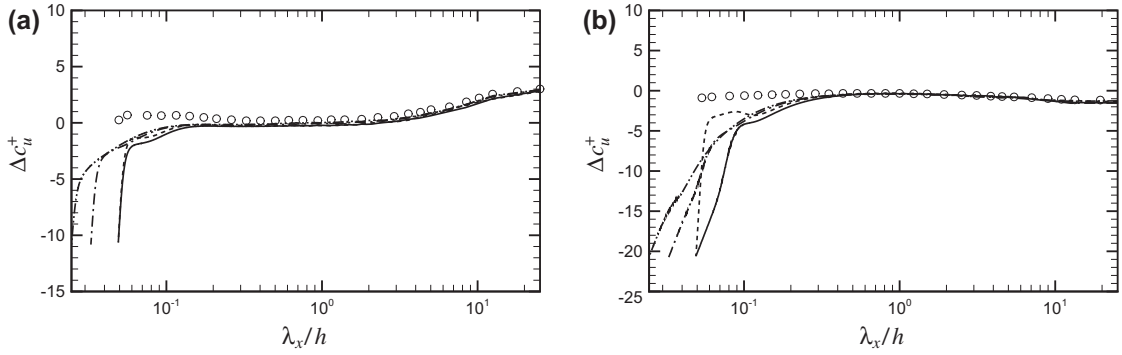


Fig. 2. Channel flow simulations in the laboratory frame: spectral distribution of the difference (Δc_u) between the convection velocity of u' and the mean velocity profile at $y^+ = 15$ (a) and $y/h = 0.75$ (b), as a function of the streamwise wavelength of the disturbances, λ_x . Solid line, Run 1; dash-dot line, Run 2; dash-dot-dot line, Run 3; dashed line, Run 4; open circles, spectral data [3].

[9]. However, the method here employed is inherently non-dissipative, and the damping of the high-frequency content has to be ascribed to other causes. In this respect it is worth noticing that the spectral densities taken in the spanwise direction (shown in panels b,d) apparently do not suffer from the same problem, and they are in good agreement (which is very good for the finer grids) with the reference data.

The misrepresentation of the smallest scales is not limited to the incorrect prediction of the streamwise spectra, but it also extends to the convection velocities of the disturbances, whose distribution is shown in Fig. 2 for the streamwise velocity component, as a function of the streamwise wavelength λ_x . While the convection velocity of a generic variable is usually derived from the wavenumber–frequency spectrum, here we adopt the method proposed by del Álamo and Jiménez [10], which has the advantage of using only local time derivatives from realizations arbitrarily spaced in time. According to their definition, the convection velocity of the streamwise velocity disturbances is given by

$$c_u = -\frac{\text{Im}(\hat{u}^* \partial_t \hat{u})}{k_x \langle |\hat{u}|^2 \rangle}, \quad (1)$$

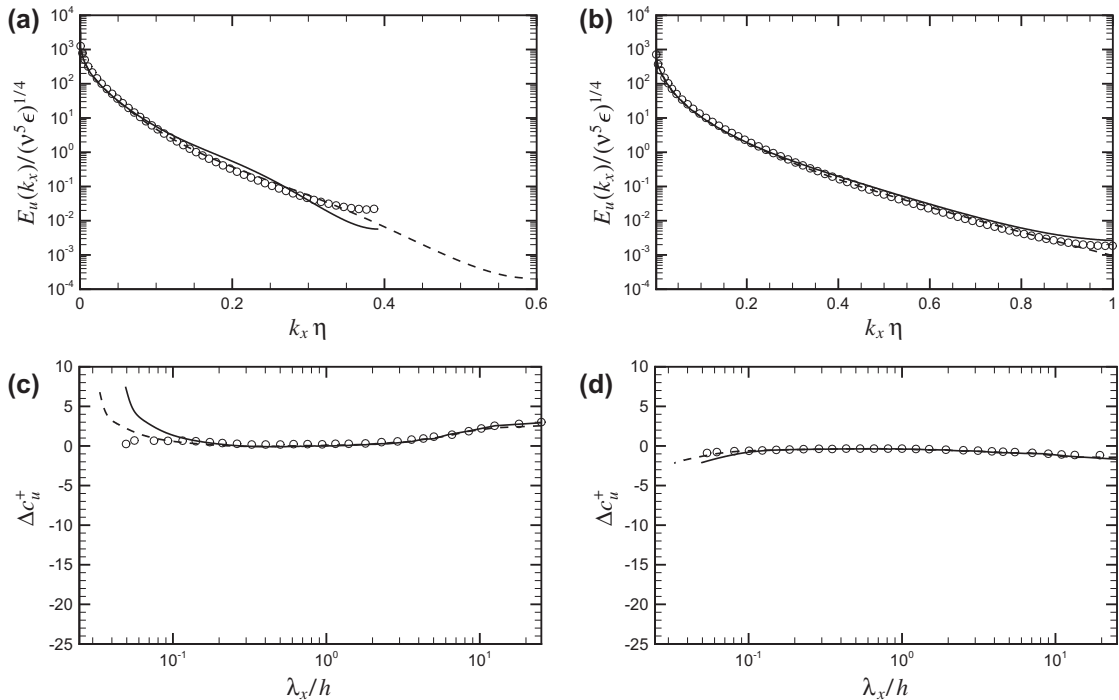


Fig. 3. Channel flow simulations in the convecting reference frame: streamwise spectral densities of streamwise velocity fluctuations (a,b) and spectral distribution of Δc_u (c,d) at $y^+ = 15$ (a,c) and $y/h = 0.75$ (b,d). Solid line, Run 1; dashed lined, Run 2; open circles, reference data [3].

where $\hat{u}(k_x, k_z, y, t)$ is the spatial Fourier coefficient of u . Fig. 2 shows c_u at two off-wall locations, as obtained from the various cases, together with the reference spectral data, in the form of deviations from the local mean velocity, which is $\bar{u}^+ = 10.6$ at $y^+ = 15$, and $\bar{u}^+ = 20.7$ at $y/h = 0.75$. Consistent with previous observations on the streamwise energy spectra, fair agreement is found (for all the simulations) with the spectral data at large scales, whereas significant differences emerge for the smallest scales, whose convection velocity is strongly underestimated by the FD solver.

As anticipated, the scope of the note is to understand the reason of the observed differences between FD and spectral methods, and devise solutions to alleviate the drawbacks of the former. For this purpose, we propose to solve the NS equations in a convecting reference frame (CRF), which moves at constant speed with respect to the laboratory frame. This strategy is not entirely new, although – to our knowledge – it was typically motivated simply by the attempt of maximizing the computational time step [see, e.g. [11]]. As discussed below, the best CRF speed is the one that minimizes the convection of disturbances across the channel. One could, for example, take the average in the wall-normal direction of the mean profile of the convection velocity of turbulent fluctuations. An operationally simpler choice is to use the bulk velocity of the flow, which approximates well the convection velocity everywhere but in the inner layer [12], and which amounts to selecting a moving frame in which the net mass flux is zero. Then, it is straightforward to think that if the total mass is zero in the streamwise direction (as for the spanwise), there could be the possibility to have a correct exponential range in the streamwise spectra.

Run 1 and Run 2 have thus been repeated in a CRF moving with the bulk flow speed ($U_b^+ = 18.3$), and the results are shown in Fig. 3. Much better agreement between the spectral and the FD data is now recovered across the whole spectral range. Some differences are still noticeable for the coarser grid at $y^+ = 15$, where the mean convective velocity is about half of the bulk velocity in the laboratory frame, and thus the convection effects are only partially removed. In this respect one should note the change of sign of the numerically computed phase speed difference between Figs. 2(a) and 3(c), which confirms a change of sign of the mean convection velocity in the moving frame. As expected, even more accurate representation of the inner layer can be achieved using a frame moving at a velocity $U_b/2$, even though the agreement in the outer layer would become somewhat poorer (the figures are omitted).

The above findings may appear quite surprising at first sight, because they apparently contradict the Galilean invariance of the NS equations. To get some insight into this behavior, we consider the one-dimensional viscous Burgers equation, which embodies several mathematical properties of the NS equations, and in particular allows for nonlinear steepening of wavefronts, with associated transfer of energy to higher wavenumbers. Let us consider the Burgers equation in a frame where the mean velocity is zero,

$$u_t + uu_x = \nu u_{xx}, \quad \int_{-\infty}^{\infty} u(x, t) dx = 0, \quad (2)$$

which describes the nonlinear advection of the u field under the action of u itself, in the absence of bulk advection. In this frame, which is the equivalent of the convecting frame in channel flow simulations, a FD semi-discretization at node j yields

$$\frac{du_j}{dt} + \mathcal{N}(u)_j = \nu \mathcal{D}_2(u)_j, \quad (3)$$

where the discrete operator \mathcal{N} symbolically denotes any possible discretization of the quadratic term, either conservative or not [8], and \mathcal{D}_2 denotes the discrete approximation of the second derivative term.

The Galilean invariance of Burgers equation implies that the governing equation are left unchanged by the change of variables $\xi = x - Ut$, $\tau = t$, $v(\xi, \tau) = u(x, t) - U$, which can be trivially verified upon substitution into Eq. (2), and which corresponds to operating in a frame of reference where the bulk velocity is U , thus being the equivalent of the laboratory frame in the channel flow simulations. However, Galilean invariance does not necessarily follow in the discrete sense. In this respect, we note that any consistent FD approximation of the nonlinear term in (2) is quadratic in the point-wise value of u . This implies that, applying the Galilean transformation to Eq. (3) yields

$$\frac{dv_j}{d\tau} + \mathcal{N}(v)_j - U \left[\left(\frac{\partial v}{\partial \xi} \right)_j - \mathcal{D}(v)_j \right] = \nu \mathcal{D}_2(v)_j, \quad (4)$$

where \mathcal{D} denotes the FD approximation of the spatial first derivative of v at node j . This equation clearly shows that the numerical method fails to discretely satisfy Galilean invariance, being different from Eq. (3), which governs the evolution of u . In particular, while the nonlinear term in Eq. (4) is identical to Eq. (3), an extra term appears, which is related to the (non-zero) mean value of v , and is linked to the accuracy in the approximation of the first derivative. Clearly, this extra term vanishes if h is reduced, and hence Galilean invariance is restored in the continuous limit. Momentarily disregarding the effect of the nonlinear and diffusive terms, spectral analysis of the approximation (4) provides [13] the evolution of a single Fourier mode $v_k(x, t) = \hat{v}(t)e^{ikx}$,

$$v_k(x, t) = \hat{v}(0)e^{ik(x - U(Z(\varphi) - \varphi)t)}, \quad (5)$$

where $\varphi = kh$ is the reduced wavenumber, and $Z(\varphi)$ is the modified wavenumber associated with \mathcal{D} . Eq. (5) indicates that the main effect of the extra term in (4) is the occurrence of a spurious drift velocity when $U \neq 0$. For instance, in the case of a

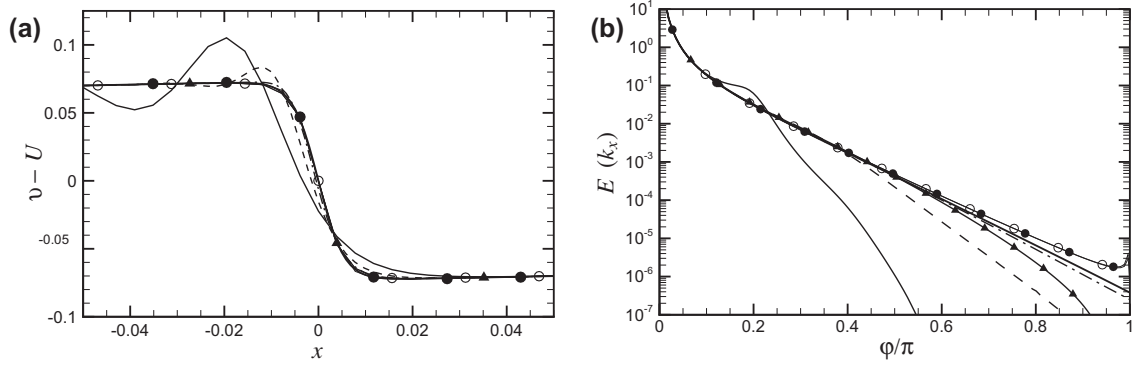


Fig. 4. Numerical solution of Burgers equation obtained with 512 (solid lines), 1024 (dashed lines), 2048 (dash-dot) collocation points. The solutions in physical space (limited to the region around the shock) are given in panel (a), and the corresponding spectra are given in panel (b). Lines without symbols indicate FD simulations in the stationary frame (i.e. $U = 1$). FD simulation in the convecting frame (i.e. $U = 0$) with 512 points is indicated with triangles. Pseudo-spectral simulations at 512 resolution are shown in the convecting frame with open circles, and in the stationary frames with closed squares. The thick solid line denotes the 'exact' solution.

second-order central-difference approximation, $(\partial v / \partial \xi)_j = (v_{j+1} - v_{j-1}) / 2h$, one has $Z(\varphi) = \sin \varphi$, and the drift velocity is negative, becoming larger in absolute value the larger is φ , i.e. for marginally resolved waves.

The main consequence of the failure of FD schemes to discretely satisfy Galilean invariance is a different behavior in the convecting and in the laboratory frames (i.e. in the case that the mean velocity is zero or not). To illustrate this change of behavior we consider Burgers equation with $v = 2 \cdot 10^{-4}$, and initial conditions $u(x, 0) = -0.1 \sin(\pi x)$, and solve it with a second-order central scheme in a frame with $U = 0$ (the convecting frame), and in a frame with $U = 1$ (the laboratory frame). The results of simulations performed in a periodic $[-1 : 1]$ domain are shown in Fig. 4 at the time $t = 10$. In the figure we show results of a second-order, energy-consistent FD discretization, which is the equivalent of the numerical method used for studying the channel flow. As a reference, we also report results obtained with a fully de-aliased spectral Burgers solver. Three grids have been considered, with 512, 1024, and 2048 collocation points. Looking at the curves obtained with 512 collocation points, it is clear that the FD solution in the convecting frame (triangles) well reproduces the nonlinear steepening of the wavefront, whereas the solution obtained in the laboratory frame (solid line) exhibits significant dispersion of its constituent harmonics and distortion of the waveform, which limits further steepening of the wavefront. Specifically, the dispersed harmonics appear to lag behind the nominal wavefront (marked with thick solid line), which confirms that their drift velocity is negative. As anticipated, such effect is much reduced as the grid resolution is increased (dashed and dash-dotted lines). In spectral space (Fig. 4(b)) the numerical spectrum in the convecting frame exhibits the expected k^{-2} tail associated with the formation of a shock singularity, whereas the solution in the laboratory frame at the lower resolution exhibits a bump, followed by a cut-off at $\varphi \approx 0.2\pi$. In this sense, one may regard the dispersive effect of FD discretizations in a moving frame as causing a bottleneck in the energy cascade to higher wavenumbers. The same effect is much reduced at higher resolution (especially for the simulation with 2048 collocation points, which is very close to exact solution), and it is virtually absent from the spectral simulations, which have zero numerical dispersion in a linear setting, being $Z(\varphi) = \varphi$. In this case the main departure from the exact solution is some energy pile-up at the highest resolved wavenumbers. Both in the laboratory frame (open circles) and in the convecting frame (solid circles), the wavefront is correctly captured by spectral methods, and no sign of numerical dispersion is apparent.

The observations made for the one-dimensional Burgers equation are completely consistent and serve to explain those made for the channel flow simulations. Specifically, we find that FD discretizations in the laboratory frame yield under-estimation of the convection velocities, especially for the highest resolved wavenumbers. The dispersive spreading of the wavefront in turn causes a bottle-neck effect in the energy spectra. This effect is not observed in the spanwise spectra (in which direction the mean convection velocity is obviously zero), nor in spectral methods, which are inherently non-dispersive.

The main message of this paper is that a judicious selection of the computational reference frame can remove (or at least greatly reduce) some shortcomings of FD discretizations of the NS equations caused by their failure to discretely satisfy Galilean invariance. In the case of turbulent channel flow, this can be approximately achieved in a simple way by carrying out the calculations in a frame moving with the bulk flow, which yield results comparable to spectral calculations. Achieving spectral-like results in the stationary frame is also possible in principle, but an impractically large number of points is required. One further advantage of operating in a convecting frame is the possibility to use larger time steps (as also acknowledged in previous studies) while preserving accuracy.

References

- [1] P. Moin, K. Mahesh, Direct numerical simulation: a tool in turbulence research, *Ann. Rev. Fluid Mech.* 30 (1998) 539–578.
- [2] J. Kim, P. Moin, R. Moser, Turbulence statistics in fully developed channel flow at low Reynolds number, *J. Fluid Mech.* 177 (1987) 133–166.

- [3] J. del Álamo, J. Jiménez, P. Zandonade, R. Moser, Scaling of the energy spectra of turbulent channels, *J. Fluid Mech.* 500 (2004) 135–144.
- [4] S. Pirozzoli, M. Bernardini, P. Orlandi, Large-scale motions and inner/outer layer interactions in turbulent Couette–Poiseuille flows, *J. Fluid Mech.* 680 (2011) 534–563.
- [5] H. Choi, P. Moin, J. Kim, Turbulent drag reduction: studies of feedback control and flow over riblets, Report TF 55, Thermosci. Div. Mech. Eng., Stanford University, 1992.
- [6] R. Kristoffersen, H. Andersson, Direct simulations of low-Reynolds-number turbulent flow in a rotating channel, *J. Fluid Mech.* 256 (1993) 163–197.
- [7] A. Kravchenko, P. Moin, On the effect of numerical errors in large eddy simulations of turbulent flows, *J. Comput. Phys.* 131 (1997) 310–322.
- [8] P. Orlandi, *Fluid Flow Phenomena: A Numerical Toolkit*, Kluwer, 2000.
- [9] M.M. Rai, P. Moin, Direct simulations of turbulent flow using finite-difference schemes, *J. Comput. Phys.* 96 (1991) 15–53.
- [10] J. del Álamo, J. Jiménez, Estimation of turbulent convection velocities and corrections to Taylor's approximation, *J. Fluid Mech.* 640 (2009) 5–26.
- [11] A. Lundbladh, S. Berlin, M. Skote, C. Hildings, J. Choi, J. Kim, D. Henningson, An efficient spectral method for simulation of incompressible flow over a flat plate, Tech. Rep. TRITA-MEK 1999:11, Dept. of Mechanics, Royal Institute of Technology, KTH, Stockholm, 1999.
- [12] M. Quadrio, P. Luchini, Integral spacetime scales in turbulent wall flows, *Phys. Fluids* 15 (2003) 2219–2227.
- [13] R. Vichnevetsky, J.B. Bowles, *Fourier analysis of numerical approximations of hyperbolic equations*, SIAM, Philadelphia, 1982.